Journal of Materials and Environmental Sciences
ISSN : 2028-2508
CODEN : JMESCN

J. Mater. Environ. Sci., 2018, Volume 9, Issue 4, Page 1223-1233

https://doi.org/10.26872/jmes.2017.9.4.134

http://www.jmaterenvironsci.com

Characterization Of Calcareous Deposits In Ground Water By Impedance Technique And Fast Controlled Precipitation Method

Hadda Semineras, Samira Ghizellaoui

Département de chimie, Faculté des Sciences Exactes, Université Des Frères Mentouri Constantine, Algérie.

Received 09 Jul 2017,
Revised 09 Sep 2017,
Accepted 15 Sep 2017

Keywords

- ✓ Calcium carbonate;
- ✓ Scaling;
- ✓ Impedancemetry;
- ✓ FCP;

Samira Ghizellaoui
gsamira@yahoo.com
+21331811177

Abstract

The calcium carbonate deposits which are observed on surface of the drains of the industrial facilities and domestic involve serious consequences. The consequences of these deposits are mainly of three types: hydraulics by obstruction partial or total of the conduits, thermals because of their bad coefficient of thermal transfer and mechanics. Various methods have been developed in order to estimate the scaling propensity of natural waters, electrochemical methods, thermal or chemical methods. This study investigate the influence of two scale inhibitors K_2HPO_4 and K_3PO_4, introduced in Hamma hard water, on the calcareous deposit formation, which is monitored by electrochemical impedance spectroscopy (EIS) and Fast controlled precipitation method (FCP). The deposits formed are analyzed by X-ray diffraction and Raman spectroscopy analyses.

1. Introduction

Calcium carbonate ($CaCO_3$) scaling is one of the most important and serious poblems in the natural water supply of industrial plants. The precipitation and crystallization of calcium carbonate as an insulating layer cause a decrease in the flow rate in pipes and reduced heat transfer in heat exchangers [1, 2]. Several chemical and electrochemical treatments exist to inhibit scale from hard water [3-5]. Scale formation can be effectively controlled by dosage of antiscalants. The most common antiscalants are polymeric organic compounds, usually phosphonates or polyelectrolytes [1]. Low concentrations of these antiscalants influence the kinetics of nucleation and crystal growth [6-10]. They can prevent the precipitation of scale forming salts by adsorption on the crystallization surface, acts to delay nucleation, reduce the precipitation rate, and modify the surface of those crystals which do form [1,11].

In this work, the inhibition of calcium carbonate precipitation by two scale inhibitors K_2HPO_4 and K_3PO_4 was studied. The efficiency of these inhibitors on $CaCO_3$ precipitation from Hamma water was determined by an electrochemical impedance spectroscopy (EIS) and fast controlled precipitation method (FCP). The precipitate morphology was analyzed by X-ray diffraction and Raman spectroscopy analyses.

2. Experimental details

2.1. Water studied

The drilling of Hamma represent a significant water resources that supply most of the city of Constantine to drinking water, physicochemical analysis is in Table 1.

It should be noted that the water of Hamma is naturally rich in minerals. Moreover, it contains calcium and magnesium. Therefore, it is of high hardness.

2.2. Electrochemical techniques

The study of scaling electrochemical phenomenon is based on accelerated scaling tests. The principle is as described by Lédion et al.(1985) [2] and Leroy et al. (1993) [12]. The scaling accelerated by electrochemical techniques consists of the forced precipitation of calcium carbonate on the surface of an electrode carried to a negative potential about (-1V) compared to a reference electrode.

Table 1: Analyzed water.

Parameter	value
T, °C	30
pH	7.09
EC, mS/cm	1.06
O_2 dissolved, mg/L	7.55
HCO_3^-, mg/L	312
TH, °F	59
Ca^{2+}, mg/L	158
Mg^{2+}, mg/L	42
Cl^-, mg/L	125
NO_3^-, mg/L	7.09
SO_4^{2-}, mg/L	127
Na^+,mg/L	116
K^+,mg/L	2.84
PO_4^{3-}, mg/L	1.63
RS ,mg/L	829

The application of this negative potential entrained to the surface of metal, they following electrochemical reaction:

$$O_2 + 2H_2O + 4e^- \longrightarrow 4OH^- \qquad R_1$$

Thus, in the vicinity of the electrode [13]. it will have an increase in the pH due to the generation of ions OH^- and involving the CO_3^{2-} formation according to the reaction:

$$HCO_3^- + OH^- \longrightarrow CO_3^{2-} + H_2O \qquad R_2$$

The product (Ca^{2+}) (CO_3^{2-}) increases and there is precipitation of $CaCO_3$ on the electrode.

$$OH^- + Ca^{2+} + HCO_3^- \longrightarrow CaCO_3(s) + H_2O \qquad R_3$$

The electrochemical measurements were obtained using a three-electrode: platinum electrode. The working electrodes were steel XC10 with 1.003 cm^2 area. The steel surface was polished with silicon carbide paper (P400). The saturated calomel electrode (SCE).The volume of water is 400 ml. The solution under stirring (700 tr/min) using a magnetic stirrer. Electrochemical experiments were driven under potentiostatic conditions using RADIOMETRE PGP 201 interface (Potentiostat/ Galvanostat (PG)) at -1 V/SCE controlled by a microcomputer. Measurements of electrochemical impedance of the interface of the 3 electrode are taken with interval of frequency ranging between 100 KHz at 100 MHz with a disturbance of 20 mV.

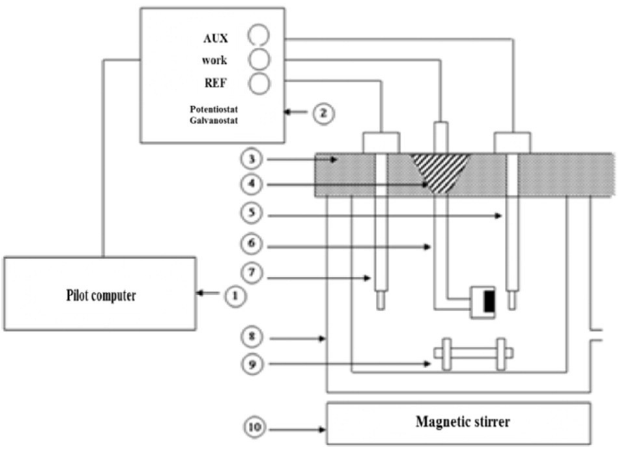

Figure 1: Experimental setup. 1 - Pilot computer 2 - Potensiostat-galvanostat 3 - Cover electrode holder 4 - Cap sample holder 5 - Platinum electrode 6 - Sample: steel pelle XC10 (1.003 cm) embedded in an inert resin 7 - Reference electrode Calomel saturated KCl 8 - Glass beaker of 600 mL 9 - Magnetic bar 10 - Magnetic stirrer.

The measurement of the electrochemical impedance shows that characterizes overall coating thickness, compactness and adhesion to the electrode [16]. Some important electrochemical parameters can be taken from the impedance diagram [4].
The resistance values of the electrolyte Re (high frequency limit $\omega \rightarrow \infty$), the polarization resistance Rp (calculated from the low frequency resistance, Rlf, Rp = Rlf - Re). The charge transfer resistance Rct (obtained by the intersection of the high-frequency half-circle with the axis of the reels). The double layer capacitance Cd (calculated from the frequency f_0, frequency at the top of the high frequency circle) :

$$2\pi f_0 R_{ct} C_d = 1$$

Where f_0 is the frequency at the top of the kinetic control loop (Figure 2).

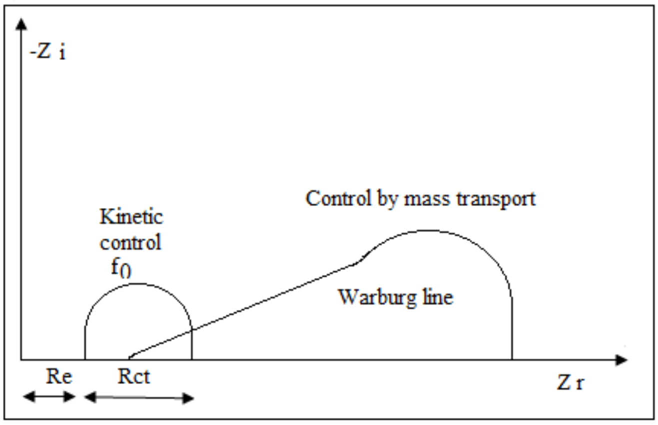

Figure 2: Theoretical Impedance Diagram.

2.3. The Fast Controlled Precipitation (FCP)
According Lédion et al. (1997) [14], to accurately characterize the scaling power of the water; the test principle is to bring the degree of supersaturation between 20 and 30. Do this by stirring promoting degassing of CO_2 dissolved in water; there is increase in the pH (H^+ ion consumption) due to the increase in OH^- ions formed by result. There producing CO_3^{2-} ions which react with Ca^{2+} to form $CaCO_3$.
These tests make it possible to follow the kinetics of the process of nucleation - growth of calcium carbonate in specific water. It compares the scaling power of waters of different origins. Thus recovering a treated water sample by K_2HPO_4, K_3PO_4 and a raw water sample, which are then brought to the same temperature 30 ° C in a thermostated bath. We are adjusted to the same volume (400 ml). It then identifies the initial values pH by a pH meter (pH Meter JENWAY 3520 equipped with a saturated calomel electrode and a temperature sensor) and resistivity by a conductivity meter (JENWAY 4520 conductivity meter equipped with a cell conductivity with integrated temperature sensor. At a given temperature, the treated water and the reference water (untreated) were stirred simultaneously at a speed of 800 tr/min. Frequencies taken of pH and resistivity are also identical for both water every 5 minutes. The whole experiment normally lasted above 100 minutes (Figure 3).

Evaluation of the efficacy of treatment
The effectiveness of any anti-scaling treatment results in retardation to precipitation. After a period of growth due to CO_2 degassing, pH decreases when precipitation begins. The subsequent decrease in pH does not follow the growth phase so precise. This is why the measurement of the resistivity takes over.
As the efficacy of a treatment should integrate all nucleation - growth phenomenon, is then determined for the same time, the ratio between the area between the two resistivity curves (treated - untreated) and the corresponding area the variation of the resistivity of the untreated water. The efficiency, *E*, was then defined by:

$$E(\%) = \frac{\int_0^t (\rho_{NT} - \rho_0)dt - \int_0^t (\rho_T - \rho_0)dt}{\int_0^t (\rho_{NT} - \rho_0)dt} 100$$

where ρ_0 : initial resistivity; ρ_{NT}: resistivity of the untreated water and ρ_T: resistivity of treated water

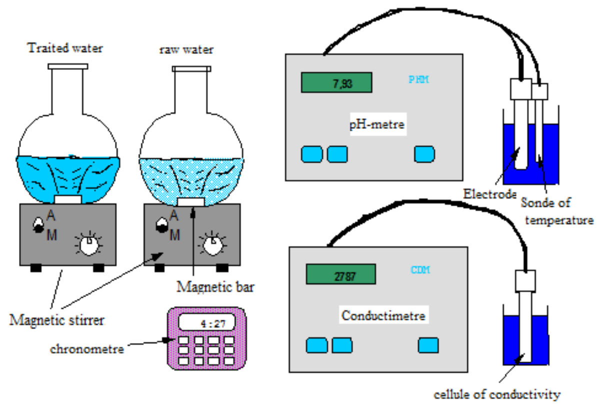

Figure 3: Experimental setup used in the Fast Controlled Precipitation (FCP) set up.

3. Results and Discussion

3.1. Impedance measurements

3.1.1 Raw water of Hamma

Impedance measurements have been used successfully to evaluate the adherence and the capacity of scale deposit on a metal electrode [15, 16]. For characterize the adhesion and compactness of the deposit of calcium carbonate. Two parameters must be considered and that can have an impedance diagram.

Rct: Charge transfer resistance.

Cd: high frequency capacity or double layer capacity.

The impedance diagrams of raw Hamma waters at 30 °C, plotted in Figure 4. Two well resolved loops are plotted. one loop, at high frequency, is due to activation (the charge transfer process) and one, at low frequency, is due to convection (the diffusion process of oxygen) [17, 18]. The diffusion of the dissolved oxygen occurs in the bulk solution and, due to the porous structure of the deposit, through the pores between the crystals blocks [19]. But when the interface is totally covered by a coherent scale the diffusion of the dissolved oxygen in the bulk solution became neglected [20, 18].

It should be noted, an important value for charge transfer resistance (Rct).Water Hamma, it is 14.62 KΩ resulting from the formation of a layer of a compact limestone deposit non-conductive and highly resistant to diffusion. The low high-frequency capacitance value for raw water Hamma (C_d = 69.96 nF/cm^2) is due to the presence of a thick scale layer on the steel electrode and the surface covered by an increasing deposit blocking and compact.

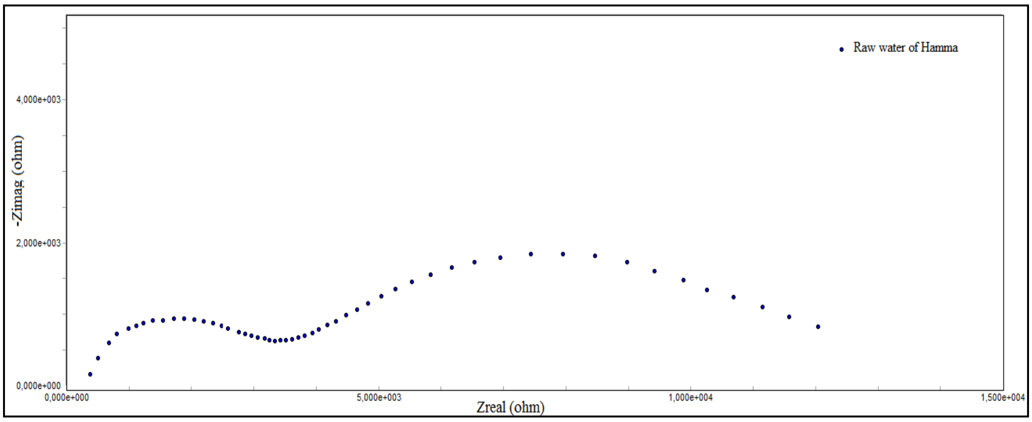

Figure 4: Impedance diagram obtained for raw water from Hamma.

3.1.2. Impedance of treated water of Hamma with K_2HPO_4

We also followed the evolution of deposits on the working electrode after 60 minutes of electrodeposition in Hamma water containing different concentrations of K_2HPO_4 by E = -1V/ SCE impedance measurements (Figure 5).

It should be noted that the shape of the diagrams is dependent on the amount of K_2HPO_4 added. The second loop obtained at low frequencies which corresponds to the process of diffusion of oxygen from raw Hamma waters has disappeared. When adding 0.1 mg/L K_2HPO_4 to Hamma water. The diameter of the charge transfer loop decreases as the concentration of K_2HPO_4 increases.

The charge transfer resistance is decreased according to the added amount of K_2HPO_4 and relative to the raw water (14.62 kohm.cm^2 for Hamma) (Table 2). This shows that when the K_2HPO_4 is added, the surface of the electrode has not been completely covered by the deposit of calcium carbonate. This is the formation of a non-conductive layer, electrically insulating less and less compact.
According to Hui and Lédion (2002) [5], the higher the charge transfer resistance, the more compact and adherent the scale deposition is the lower the charge transfer resistance is related to the diffusion of oxygen in the solution. As a result of an increase in the C_{HF}, the $CaCO_3$ recovery rate of the metal surface decreases (Table 2). The determination of the capacity values in the high frequency (Cd), therefore, makes sense to follow the free metal surface if the limestone is deposited. Cd increases as the concentration of K_2HPO_4 increases.

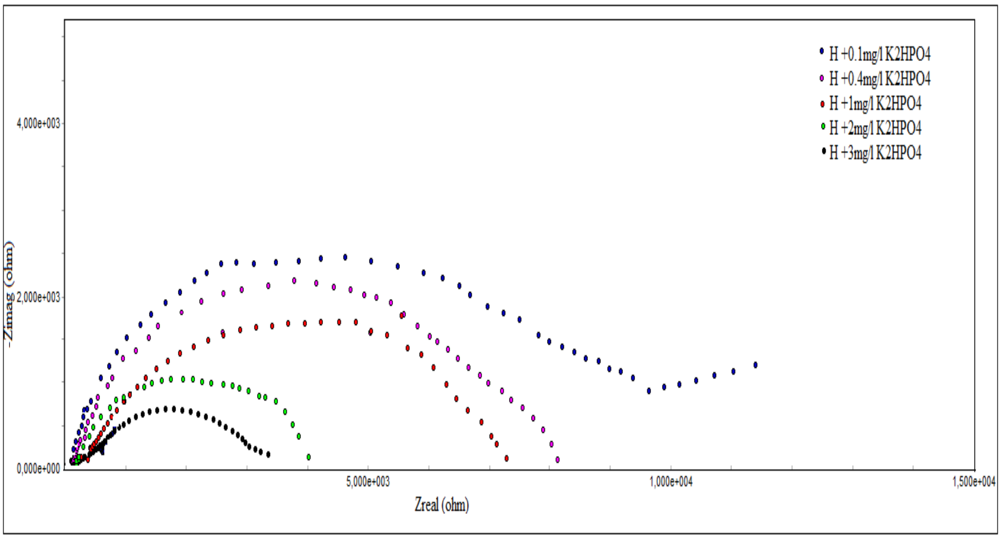

Figure 5: Impedance diagrams obtained for treated water of Hamma at different concentrations of K_2HPO_4 (T=30°C).

Table 2: Charge transfer resistance (Rct), double layer capacity (Cd) and efficiency for treated water at different concentrations of K_2HPO_4.

Concentration (mg/L)	C_d (µF/cm^2)	R_{ct} (kohm.cm^2)
00	0.069	14.62
0.1	0.102	8.03
0.4	1.65	5.91
1	5.86	4.99
2	9.07	3.75
3	33.4	1.78

3.1.3. Impedance of treated water of Hamma with K_3PO_4
Mass transfer control is only observed in the case of raw water. On addition of 0.1 mg/L K_3PO_4 water Hamma diffusional branch disappears (Figure 6).

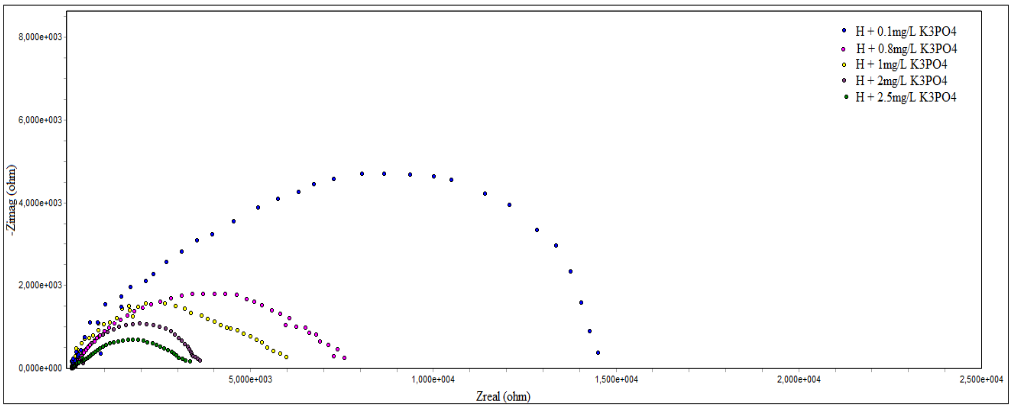

Figure 6: Impedance diagrams obtained for treated water of Hamma at different concentrations of K_3PO_4 (T=30°C).

The measurement of impedance of water treated by K_3PO_4 showed that the deposition of calcium carbonate decreases, this is verified by the increase of the high frequency capacity (Cd) and decreased charge transfer resistance (Rct) as a function of the increased concentration of K_3PO_4 added (Table 3).

Table 3: Charge transfer resistance (Rct), double layer capacity (Cd) and efficiency for treated water at different concentrations of K_3PO_4.

Concentration (mg/L)	C_d ($\mu F/cm^2$)	R_{ct} ($kohm.cm^2$)
00	0.069	14.62
0.1	0.032	14.24
0.8	1.065	4.32
1	15.86	4.28
2	35.98	2.6
2.5	55.14	1.79

3.2. Effect of inhibitors concentrations evaluated by FCP method

Figure 7-9 show the shape of the PCR curves of the raw water of the Hamma relative to the water treated with (K_2HPO_4, K_3PO_4). There are three distinct phases.

Initially, there was an increase in pH: the degassing of CO_2 which predominates over the precipitation of $CaCO_3$, since a sufficiently high degree of supersaturation (δ <40) has not been reached, generates an ion consumption. In a second step, the pH tends to decrease due to the precipitation of the calcium carbonate which takes precedence over the degassing according to the reaction:

$$Ca^{2+} + CO_3^{2-} \rightleftharpoons CaCO_3\ (s)$$

In a third stage, the degassing of CO_2 and the precipitation of the $CaCO_3$ tend to balance, so a stabilization of the pH is observed.

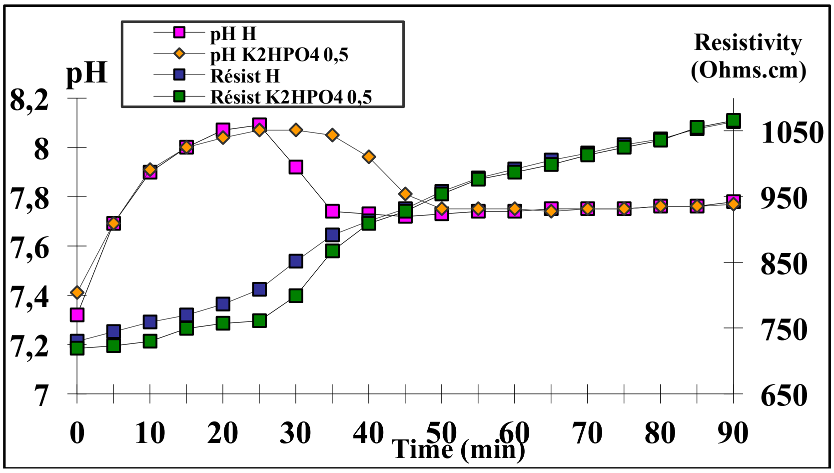

Figure 7: FCP curves of treated Hamma water with 0.5 mg/L of K_2HPO_4.

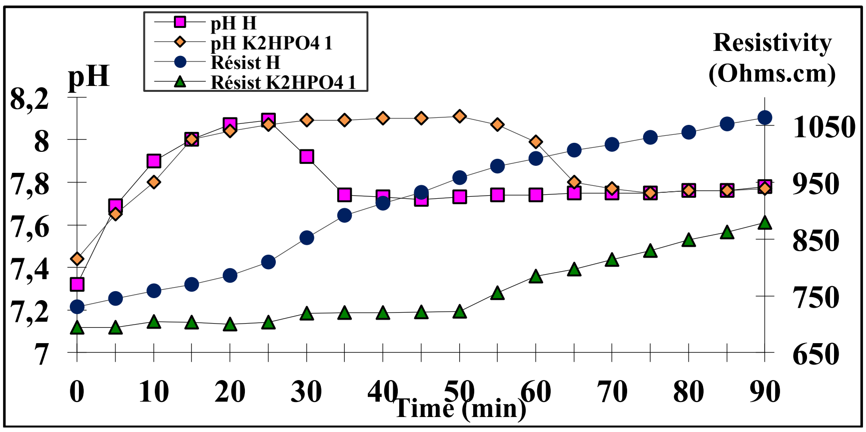

Figure 8: FCP curves of treated Hamma water with 1 mg/L of K_2HPO_4.

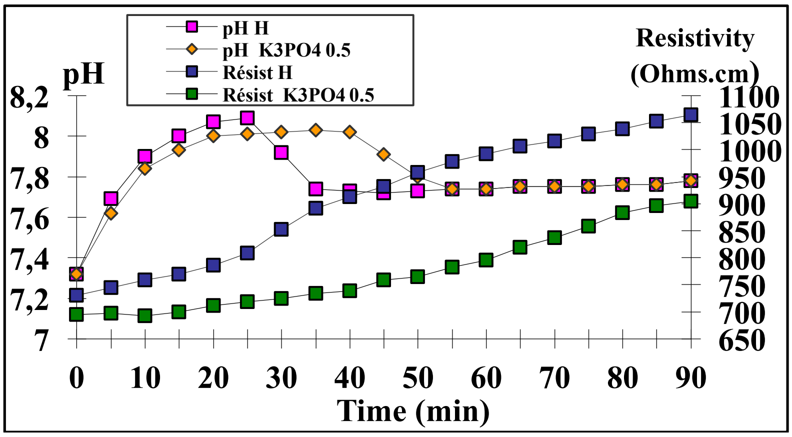

Figure 9: FCP curves of treated Hamma water with 0.5 mg/L of K_3PO_4.

The pH of the raw water generally decreases before that of the treated water (delay in precipitation) and decreases more rapidly (difference in precipitation kinetics) when scaling inhibitors are used.
The pH of the raw water decreases after reaching a maximum value, which corresponds to a precipitation pH value (pHp = 8.05). The precipitation time (tp) corresponds to the time associated with the maximum value of pHp [21]. This evolution indicates a precipitation of calcium carbonate at (tp = 25 min), the resistivity for the raw waters increases strongly and linearly. Table (4-5).
For the treated water the precipitation of $CaCO_3$ is delayed. The precipitation time increases with the concentration of inhibitors Tables (4-5). The homogeneous precipitation of $CaCO_3$ is delayed when the inhibitor is added. With the addition of 2.5m /L K_2HPO_4, 2mg/L K_3PO_4, the appearance of the curve changes with no precipitation, which translates the total inhibition of $CaCO_3$ Figures (10-11).

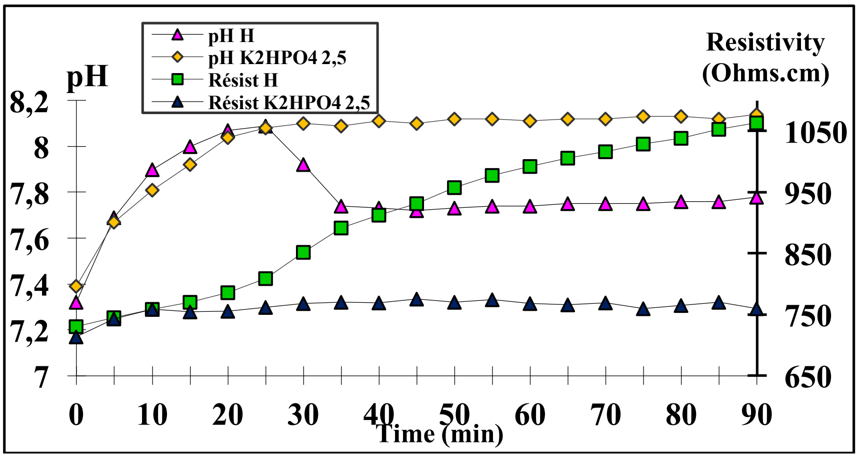

Figure 10: FCP curves of treated Hamma water with 2,5 mg/L of K_2HPO_4.

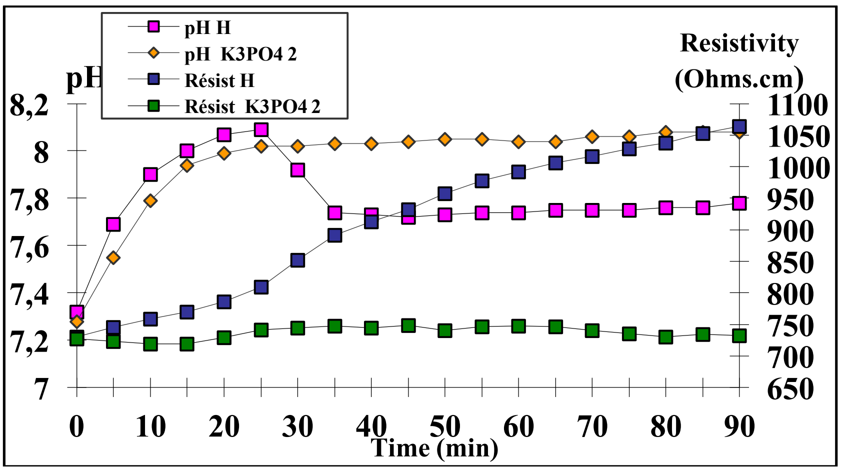

Figure 11: FCP curves of treated Hamma water with 2mg/L of K_3PO_4.

Table 4: pHP, tP for the Hamma waters treated with K_2HPO_4.

	Concentration (mg/L)	pH_P	t_P(min)
Water of the Hamma	0	8.09	25
	0.5	8 .05	35
	1	8.11	50
	1.5	8.11	60
	2	-	-
	2.5	-	-

Table 5: Table 30: pHP, tP for the Hamma waters treated with K_3PO_4.

	Concentration (mg/L)	pH_P	t_P(min)
Water of the Hamma	0	8.09	25
	0.25	8 .02	30
	0.5	8.02	40
	1	8.05	55
	1 .5	8.04	70
	2	-	-

The germination and growth processes can also be determined by an analysis of the resistivity curve. Indeed, when there is precipitation, therefore consumption of ions (Ca^{2+}, CO_3^{2-}, H^+ …), and a decrease in conductivity is observed, hence an increase in resistivity. An anti-scale treatment causes a delay in precipitation, which is why the resistivity of the treated water increases only after that of the untreated water and on the other hand slows down the precipitation kinetics (lower carbonate production of calcium). No precipitation of $CaCO_3$ occurred for 2.5mg /L K_2HPO_4, 2mg /L K_3PO_4 no decrease in pH values and resistivity remains constant over time and the curve shape changes for high efficiency. These results indicate that the inhibitor concentration could completely inhibit $CaCO_3$ precipitation.
With an addition of 1 mg/L of K_2HPO_4 the efficiency reaches 67% and from 2 mg/L the blocking of the (germination - growth) process of calcium carbonate is more important and for the same addition of K_3PO_4 to of the Hamma water, the efficiency is 71% and the total blockage of the (germination - growth) of $CaCO_3$ starts from 1.5 mg/L. 100% efficiency was achieved with total blockage of growth-germination for addition of 2.5 mg/L of K_2HPO_4 and 2 mg/L of K_3PO_4 to Hamma water (Figure 12). K_3PO_4 is more efficient as antiscalant than K_2HPO_4. This inhibitor adsorbe on the active sites of the crystals of calcium carbonate.

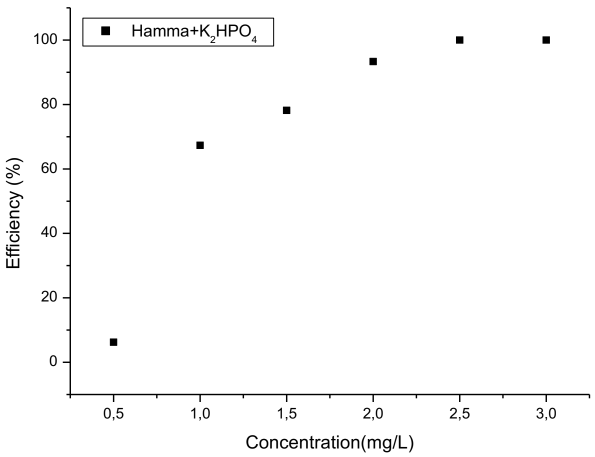

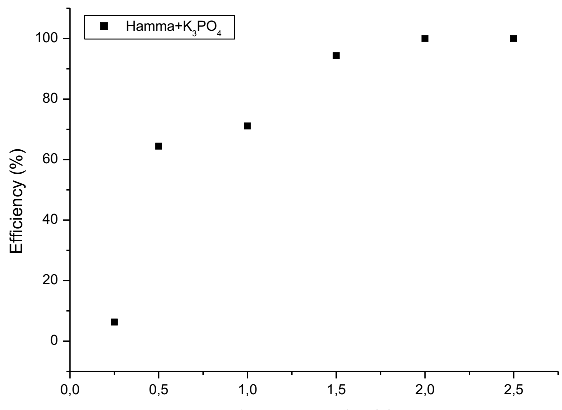

Figure 12: Evolution of the efficiency as a function of the concentration of K_2HP0_4 and K_3P0_4 in Hamma water.

3.3. XRD and Raman spectroscopic analysis

Characterization of the deposition of the raw water Hamma by X-ray diffraction indicates that the salt formed is composed of calcium carbonate, which crystallizes in two varieties crystallographic calcite and vaterite Predominantly calcite phase (Figure 13). the calcium carbonate precipitates in the form of calcite in raw water and in the presence of a very low concentration of K_2HPO_4 and K_3PO_4 change the morphology of the calcium carbonate of the calcite to vaterite and aragonite form (Figure 14,15).

It is well known that calcite is the most thermodynamically stable and vaterite the least stable form in the three polymorphic forms of $CaCO_3$ [21-23]. Vaterite is the initial phase formed in $CaCO_3$ supersaturated, calcite can be formed from the transformation of aragonite or vaterite in the absence of inhibitors Although calcite has the greatest thermodynamic stability under ambient conditions, the thermodynamically less stable aragonite and/or vaterite phase may be stabilized under certain conditions of temperature or in the presence of other ions or inhibitors [24].

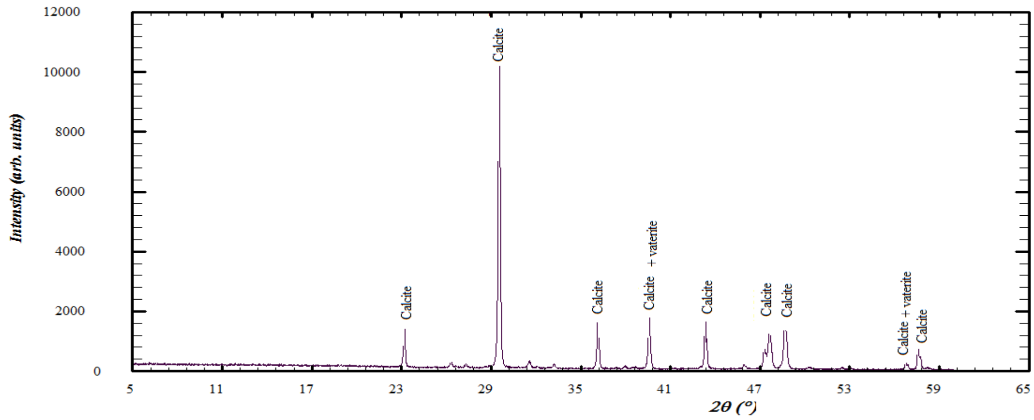

Figure 13: The XRD pattern of the $CaCO_3$ scale deposition of water Hamma.

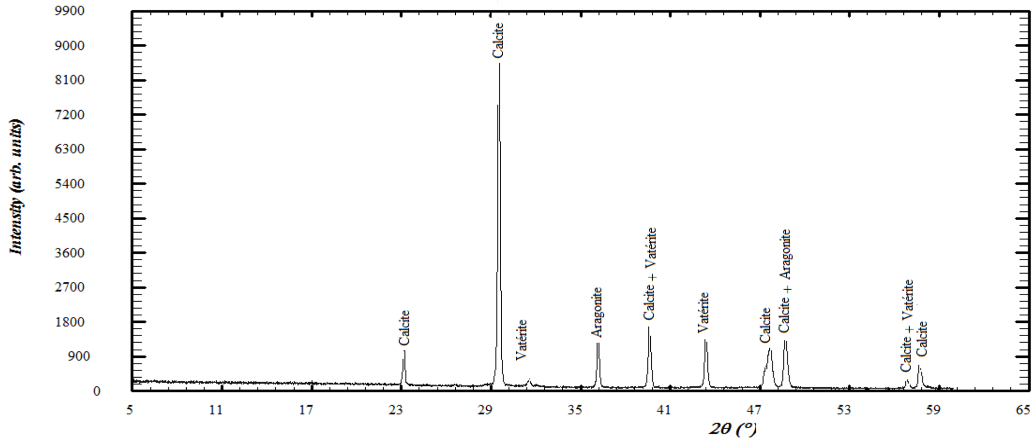

Figure 14: The XRD pattern of the $CaCO_3$ scale deposition of water Hamma treated with 0.5mg/L K_2HPO4.

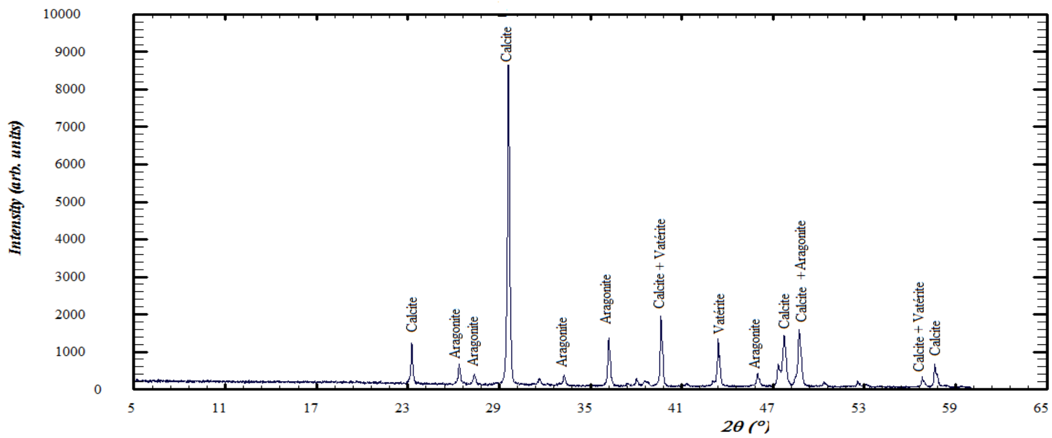

Figure 15: The XRD pattern of the $CaCO_3$ scale deposition of water Hamma treated with 0.5mg/L K_3PO4.

The above results were further confirmed by Raman spectroscopy the characteristic symmetric stretching band at 1085 cm^{-1}, the lattice modes at 154 cm^{-1} with overlapping band at 281 cm^{-1} and band at 711 cm^{-1} confirmed the presence of calcite in the absence of inhibitors (Figure 16). In the presence of inhibitors, their crystallization is in the form of a mixture of three crystallographic varieties (calcite, aragonite and vaterite). Indeed, they have peaks at 155, 282, 1087 cm^{-1}, characteristic of calcium carbonate in the aragonite crystallographic form. The peaks at 212 and 750 cm^{-1}, characteristics of calcium carbonate in the crystallographic vaterite form Figures (17, 18).

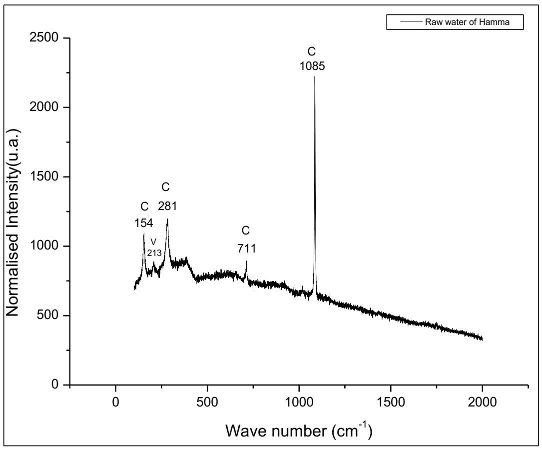

Figure 16: Raman spectra of Hamma raw water.

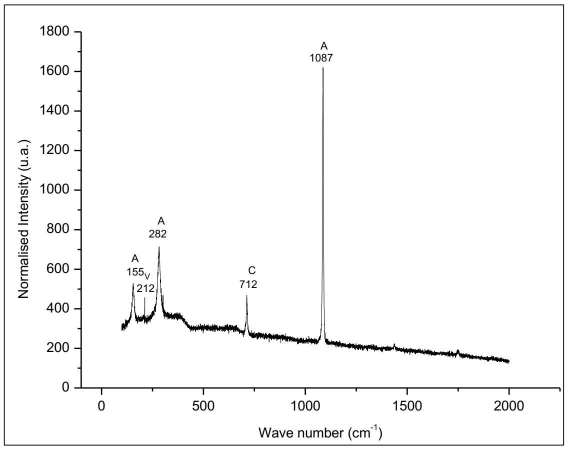

Figure 17: Raman spectra of precipitated scale products in presence of 0.5mg/L of K_3PO_4.

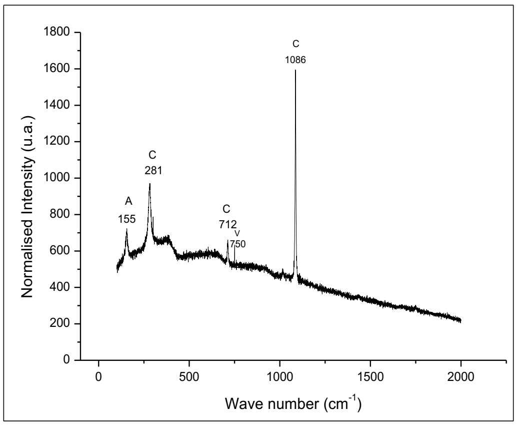

Figure 18: Raman spectra of precipitated scale products in presence of 0.5mg/L of K_2HPO_4.

Conclusion

The main objective of this study is to inhibit the scaling power of Hamma hard waters by using a K_2HPO_4, K_3PO_4.

We carried out measurements of the impedances of the scale deposits of the raw waters of Hamma and treated with inhibitors. The method has shown that the charge transfer resistance (Rct) decreases and the high frequency capacitance (Cd) evolves as a function of the concentration of addition of each inhibitor, confirming the effectiveness of the antiscalant action of the inhibitors used. The presence of K_2HPO_4 or K_3PO_4 at low concentration 2.5 mg/L of K_3PO_4 and 3 mg/L of K_2HPO_4 reduced the surface coverage of deposits on the electrode and the scaling rate.

The use of the fast controlled precipitation method (FCP) allowed us to follow the kinetics of the germination process - growth of calcium carbonate as well; we have demonstrated the retarding effect of inhibitors. The precipitation of $CaCO_3$ in solution was totally inhibited for 2 mg/L of K_3PO_4 and 2.5 mg/L of K_2HPO_4.

In the presence of these inhibitors in water, we have shown that the calcium carbonate deposit changes morphology of the calcite form in the raw water and becomes in the form of a mixture of calcite, vaterite and aragonite.

References

1. K. Zeppenfeld, *Desalination*. 252 (2010) 60-65.
2. C. Duffau, C. Gabrielli, A. Sandra, *L'Eau, l'Industrie, les Nuisances.* 186 (1995) 50-55.
3. J. Ledion, P. Leroy, J.P. Labbe, *TSM L'eau.* (1985) 323-328.
4. W. Lin, C. Colin, R. Rosset, *TSM L'eau* 85, N^0 12 (1990) 613-620.

5. F. Hui, J. Ledion, *Eur. j. water qual.* 33 (2002).
6. L. Yi-Pin, C. Philip, *Water. Res.*39 (2005) 4835-4843.
7. Z. Liu, Y. Sun, X. Zhou, T. Wu, Y. Tian, Y. Wang, *J. Environ. Sci.* 23 (2011) 153-155.
8. D.E. Abd-El-Khalek, B. Abd-El-Nabey, *Desalination.* 311 (2013) 227-233.
9. Y. Boulahlib-Bendaoud, S. Ghizellaoui, *J. Mater. Environ. Sci*. 6 (2) (2015) 307.
10. H. Semine Ras, S. Ghizellaoui, *J. Mater. Environ. Sci*. 6 (2) (2015) 377.
11. S. Ghizellaoui, M. Euvrard, J. Lédion, A. Chibani, *Desalination.* 206 (2007) 185-197.
12. P. Leroy, J. Lédion, A. Khalil, *Aqua.* 42(1991) 23-29.
13. M. Zidoune, A. Khalil, P. Sakya, C. Colin, R. Rosset, *Electrochimie. C. R. Acad. Sci. Paris, t.* 315 (1992) 795-799.
14. J. Ledion, B. François, J. Vienne, *J. Euro. d'hydrologie,* 28 (1997) 15-35.
15. F. Nguyen, *Thèse de doctorat de l'université de Paris* VI (1996) 233.
16. A. Khalil, C. Colin, C. Gabrielli, M. Kheddam, R. Rosset, *C. R. Acad. Sci, Paris.* 316 (1993) 19-24.
17. O. Devos, C. Gabrielli, B. Tribollet, Electrochim. Acta 51 (2006) 1413.
18. C. Rousseau, F. Baraud, L. Leleyter, M. Jeannin, O. Gila, *Electrochimica Acta*. 55 (2009) 196-203.
19. C. Gabrielli, M. Keddam, A. Khalil, R. Rosset, M. Zidoune, *Electrochim Acta.* 42 (1997) 1207.
20. J. Marin-Cruz, R. Cabrera-Sierra, M.A. Pech-Canul, I. González, *J. Appl. Electrochem*. 34 (2004) 337.
21. D. Peronno, H. Cheap-Charpentier, O. Horner, H. Perrot, *J. Water. Process. Eng.* 7 (2015) 11-20.
22. S. Ghizellaoui, S. Ghizellaoui, H. Semineras, *J. Mater. Environ. Sci*. 8 (2017) 2105 -2111.
23. R. Menzri, S. Ghizellaoui, M. Tlili, *Desalination.* 404 (2017) 147-154.
24. C. Wang, S. Li, T. Li, *Desalination.* 249 (2009) 1-4.

(2018) ;http://www.jmaterenvironsci.com